ARTICLE OPEN ACCESS

Heritability of cervical spinal cord structure

Linda Solstrand Dahlberg, PhD, Olivia Viessmann, PhD, and Clas Linnman, PhD

Correspondence
Dr. Linnman
clinnman@partners.org

Neurol Genet 2020;6:e401. doi:10.1212/NXG.0000000000000401

Abstract

Objective

Measures of spinal cord structure can be a useful phenotype to track disease severity and development; this observational study measures the hereditability of cervical spinal cord anatomy and its correlates in healthy human beings.

Methods

Twin data from the Human Connectome Project were analyzed with semiautomated spinal cord segmentation, evaluating test-retest reliability and broad-sense heritability with an AE model. Relationships between spinal cord metrics, general physical measures, regional brain structural measures, and motor function were assessed.

Results

We found that the spinal cord C2 cross-sectional area (CSA), left-right width (LRW), and anterior-posterior width (APW) are highly heritable (85%–91%). All measures were highly correlated with the brain volume, and CSA only was positively correlated with thalamic volumes (p = 0.005) but negatively correlated with the occipital cortex area (p = 0.001). LRW was correlated with the participant's height (p = 0.00027). The subjects' sex significantly influenced these metrics. Analyses of a test-retest data set confirmed validity of the approach.

Conclusions

This study provides the evidence of genetic influence on spinal cord structure. MRI metrics of cervical spinal cord anatomy are robust and not easily influenced by nonpathological environmental factors, providing a useful metric for monitoring normal development and progression of neurodegenerative disorders affecting the spinal cord, including—but not limited to—spinal cord injury and MS.

From the Department of Anesthesiology, Perioperative and Pain Medicine (L.S.D., C.L.), Boston Children's Hospital, Harvard Medical School, MA; Departments of Psychiatry and Radiology (L.S.D., C.L.), Massachusetts General Hospital, Harvard Medical School; Department of Neurology and Neurosurgery (L.S.D.), Montreal Neurological Institute, McGill University, Canada; Athinoula A. Martinos Center for Biomedical Imaging (O.V.), Department of Radiology, Harvard Medical School, Massachusetts General Hospital, Charlestown, Boston; and Spaulding Neuroimaging Lab (C.L.), Spaulding Rehabilitation Hospital, Harvard Medical School, Boston, MA.

Go to Neurology.org/NG for full disclosures. Funding information is provided at the end of the article.

The Article Processing Charge was funded by the authors.

Glossary

ACE = additive plus common plus nonshared environment and error model; **AE** = additive plus nonshared environment and error model; **AIC** = Akaike information criterion; **APW** = anterior-posterior width; **BMI** = body mass index; **CSA** = cross-sectional area; **DZ** = dizygotic; **HCP** = Human Connectome Project; **LRW** = left-right width; **MZ** = monozygotic; **SCI** = spinal cord injury.

Automated and semiautomated approaches have been developed to study spinal cord structure, enabling rater-independent segmentation and quantification of spinal cord metrics. Using these methods, recent studies have reported reductions in the spinal cord cross-sectional area (CSA), left-right width (LRW), and anterior-posterior width (APW) in MS,[1,2] amyotrophic lateral sclerosis,[3] and spinal cord injury (SCI).[4–8] After SCI, changes to the sensorimotor cortex have also been reported,[9,10] indicative of cortical reorganization because of the lack of afferent input from the spinal cord. Of interest, spinal cord atrophy correlates with physical functioning after SCI.[7,8] This suggests that cord atrophy may be proportional to somato-motor cortex atrophy. However, it is unknown if such a relationship exists before injury, i.e., is the spinal cord structure linked to the cortical sensorimotor representation and with motor abilities in healthy subjects?

Human brain anatomy is heritable with a genetic contribution between 66% and 97% for total brain volume, as estimated in twin studies.[11] There are no previous studies on heritability of spinal cord structure. Determining factors that contribute to variations in spinal cord structure in healthy individuals add to our understanding of the CNS and, crucially, to markers of neurodegenerative pathology.

We hypothesized that CSA, LRW, and APW of the spinal cord is (1) reliably measured, (2) hereditary, and (3) is proportional to the volume of the thalamus and cerebellum and the sensory and motor cortex area, as well as to motor function.

Methods

Data included in the analyses

Data used in the current study were a subset of unprocessed structural data from the Human Connectome Project (HCP) including test-retest data (db.humanconnectome.org). We investigated 332 participants. Sufficient brain coverage to quantify CSA was obtained in 283 participants. These were 50 pairs of monozygotic (MZ) and 50 pairs of dizygotic (DZ) twins, as well as 83 unrelated participants. MZ and DZ twin pairs were selected to be matched for age (±5 years) and race. Structural brain scans, behavioral data and information on the participants' whole brain volume (ventricles excluded), and regional brain areas and volumes (obtained by the HCP FreeSurfer parcellation[12]) were used in the subsequent analyses. Brain regions included the bilateral precentral and postcentral gyrus, and volumes of the cerebellar gray matter and thalamus. Data for all variables of interest were available for all participants.

In the HCP data set, there is test-retest data from 45 participants. Of the 45 participants, 9 were excluded because spinal cord segmentation did not work on either one or both of their scans, primarily because of poor tissue contrast or incomplete coverage of the cervical spine. Ultimately, 36 participants remained in the test-retest analysis, where the first data set was also included in the main heredity analysis. See Supplemental Data for test-retest methodology and results, links.lww.com/NXG/A225.

MRI

The HCP data were acquired at Washington University in St. Louis on a 3 Tesla Siemens Connectome Skyra scanner (Siemens, Erlangen, Germany) using a 32-channel head coil.[13] The structural scan was a T1-weighted magnetisation prepared rapid gradient echo: repetition time: 2,400 ms, echo time: 2.14 ms, inversion time: 1,000 ms, flip angle: 8°, and matrix size: 266 × 320 × 320, 0.7 mm isotropic voxel size. The 224-mm coverage along the Z direction (head to toe) allowed for evaluation of cervical structures in most participants to spinal level C2 and in some cases C3. To take advantage of the full field of view, raw MRI data from HCP were obtained and subsequently corrected gradient field nonlinearity. See supplemental data for details (links.lww.com/NXG/A225), including an evaluation of the effect of gradient field nonlinearity correction on data validity.

Spinal cord segmentation

Image processing of the spinal cord was carried out with the Spinal Cord Toolbox.[14] It used semiautomatic methods for segmentation, labeling, and extraction of spinal cord metrics. Because the HCP data are centered over the brain, manual landmarks of the spinal cord were used to initiate the detection of the cord for the subsequent automatic segmentation. The output is a binary mask of the spinal cord in 3D space that was inspected in each participant. The next step registered the data to the MNI-Poly-AMU template, including probabilistic labeling of the spinal segments of each vertebrae. The template is then warped back to native space of each participant. The fit of the template and each spinal cord segment were manually inspected in all participants. Finally, CSA, LRW, and APW were extracted from each segment of the cord. Here, we examine the C2 level of the spinal cord because the C2 level is at an ideal location for segmentation and analysis; the surrounding CSF creates optimal contrast for accurate segmentation of this area, with less curvature than that of the more caudal spinal cord levels.[15] Moreover, studies on SCI and MS have reported the C2 structure to be linked to clinical outcome scores.[16–18] If the border between 2 segments was not in accordance with landmarks surrounding the spinal cord, the slices corresponding to each level were manually selected and used in calculation of C2 CSA, LRW, and APW.

Behavioral measurements

All measurements pertaining to motor functioning were obtained with the NIH Toolbox Motor Battery.[19] We used data from the 9-hole pegboard dexterity test, the grip strength test, the 4-m walk gait speed test, and the 2-minute walk endurance test. To estimate simple reaction time, we used reaction times from the 0-back working memory task, under the assumption that the 0-back control condition would primarily reflect a direct perceptual response[20] not affected by working memory load.

Statistical analyses

Statistical analyses on the test–retest data and spine metrics and behavioral measures were carried out in GraphPad Prism version 7.0c for Mac (GraphPad Software, La Jolla, California, graphpad.com). Linear regression analyses between cord anatomical metrics, physical, behavioral, and brain metrics were carried out with the statistical package R in R Studio (RStudio: Integrated Development for R. RStudio, Inc., Boston, MA, rstudio.com/). Heritability analyses were conducted using a classic twin model carried out with the "mets" package, also implemented in R.

Relations to behavioral and brain measures

Simple regression models are not appropriate for twin data because the assumption of independence between observations is violated by the paired structure of data.[21] To determine the relationship between spinal cord metrics and behavior or brain metrics, we used multiple regression models where the mean value of twin pairs and the difference between twin pairs was used as regressors (model 2 in reference 21). Data from non-twins (n = 83) were also included in the models.

These analyses were used to investigate the relationship between CSA, LRW, and APW:

1. General physical measures: body height, body weight, body mass index (BMI), and total brain volume. Each model also controlled for the sex of the subjects. The resulting 4 separate regression models were Bonferroni corrected (4 variables, $p < 0.0125$ considered significant).
2. Motor function: grip strength (age adjusted), dexterity (age adjusted), endurance (age adjusted) and gait speed, and reaction time from the 0-back working memory task (5 variables, $p < 0.01$ considered significant).
3. Brain metrics: area of the bilateral precentral and postcentral gyrus, the volume of the cerebellar gray matter, and the volume of the thalamus. As a "control" region, we also calculated the relationship to the occipital area. Each model also controlled for sex and total brain volume (5 variables, $p < 0.01$ considered significant).

Sex as a biological variable

To evaluate if sex influenced CSA, LRW, and APW while controlling for weight and body length, 3 multiple regression models were calculated and adjusted for twin-samples as mentioned above.

Heritability analysis

To inspect data, correlations in intratwin pairs were first carried out with a Spearman rank-order correlation. A higher correlation in the MZ twins compared with the DZ twins indicates a genetic influence on the tested traits: CSA, LRW, and APW (figure 1).

Two models were initially run, an additive plus common plus nonshared environment and error model (ACE) and an additive plus nonshared environment and error model (AE) model which models the variance in 3 components: additive genetic effect (A), shared environmental effects (C), and unique environmental effects plus error (E). The model fit was estimated with Akaike information criterion (AIC), where the lowest AIC value indicates the best fitting model.

The polygenic model was carried out on CSA, LRW, and APW. Age and sex were therefore included as covariates in the analyses.

Standard protocol approvals, registrations, and patient consents

Because this study was conducted with publicly available data from the HCP (as well as HCP Restricted Access Data), consent was obtained by the HCP. Details regarding data access are found in their previously published studies (for example [reference 5]).

Data availability

The imaging data, behavioral test scores, and demographics used for this project are readily available from the HCP (db.humanconnectome.org). In accordance with the HCP Restricted Access Data Use Terms,[22] study-specific participant IDs to each individual, as well as the resulting spinal cord segmentation data, will be made available on publication through the HCP Database (db.humanconnectome.org).

Results

Demographics

We analyzed C2 CSA, LRW, and APW in 332 participants, whereof 52 participants were excluded from the analyses because of unreliable or incomplete coverage of the C2 vertebrae. The final sample (n = 283) consisted of 190 women and 93 men, with an average age of 29.5 years (range 22–36 years). There were significantly more women than men in the sample, and women were approximately 2 years younger (women = 27.9 years vs men = 30.1 years, $p < 0.0001$). Participants in the analyzed sample, consisting mostly of twins and with a higher proportion of females, were on average significantly shorter (168.5 cm vs 171.4 cm, $p < 10^{-4}$) and lighter (75.4 kg vs 79.9 kg, $p < 10^{-4}$) than the full HCP sample.

Cord metrics

The mean C2 CSA was 71.77 (±5.65) mm^2, the mean LRW was 11.52 (±0.61) mm, and the mean APW was 8.0 (±0.49) mm. LRW and APW were highly correlated with CSA values (see figure e-1, links.lww.com/NXG/A225); however, LRW and APW were not significantly correlated with each other (table e-1

Figure 1 Distribution of cervical spinal cord anatomical measures in the sample

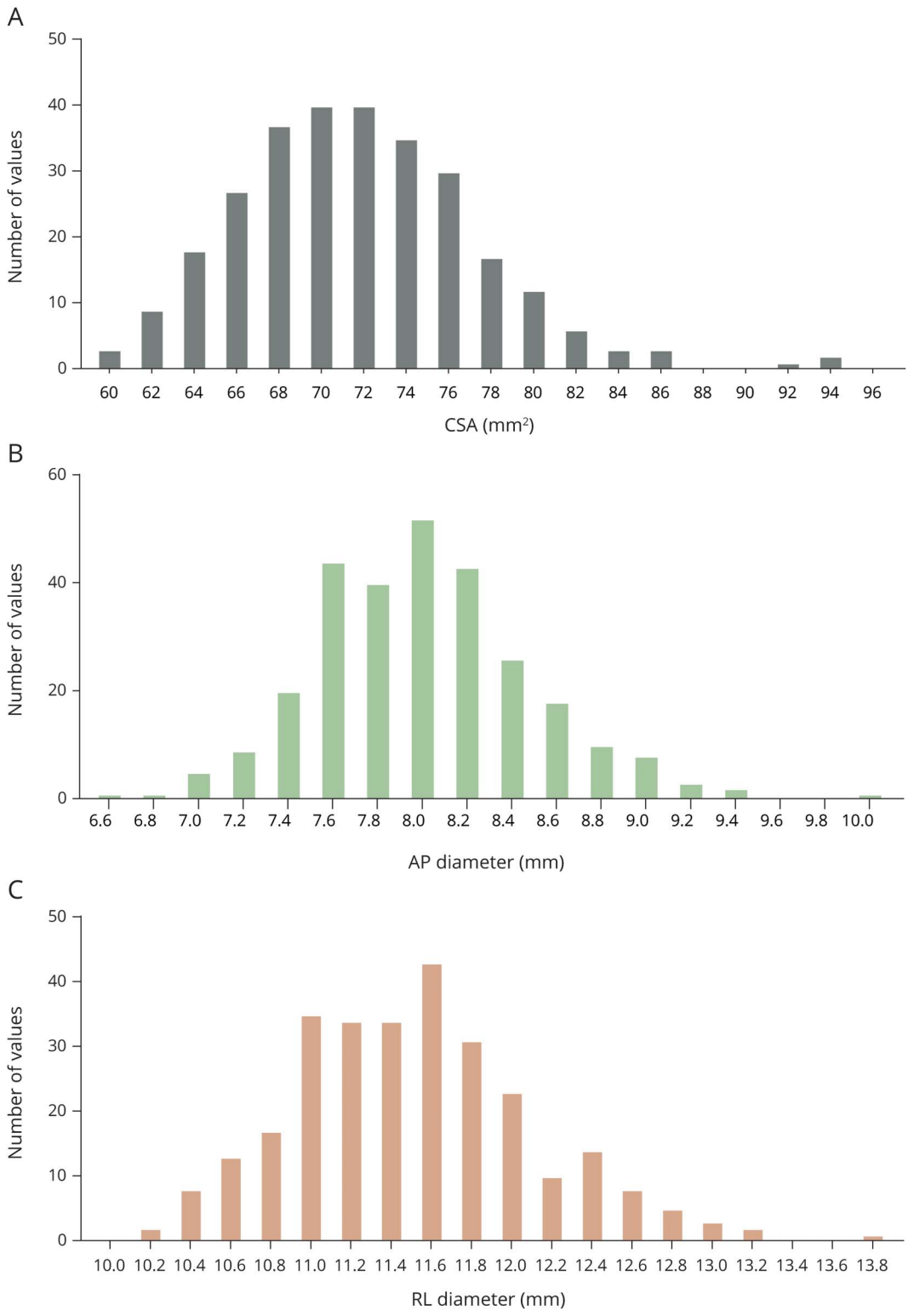

(A) CSA = cross-sectional area; (B) A-P = anterior–posterior width; (C) R-L = right–left width.

and figure e-2, links.lww.com/NXG/A225). A robust regression and outlier removal test was carried out to examine the data for outliers.[23] With the default coefficient criterion of Q = 1%, the test identified 3 outliers in the CSA measures and one outlier in APW (of which one was also an outlier in the CSA data). We chose not to exclude any of these data because a visual inspection verified that these were not products of methodological errors, rather they represent large values from the natural variability in the data.

Figure 2 C2 cross-sectional T1w image

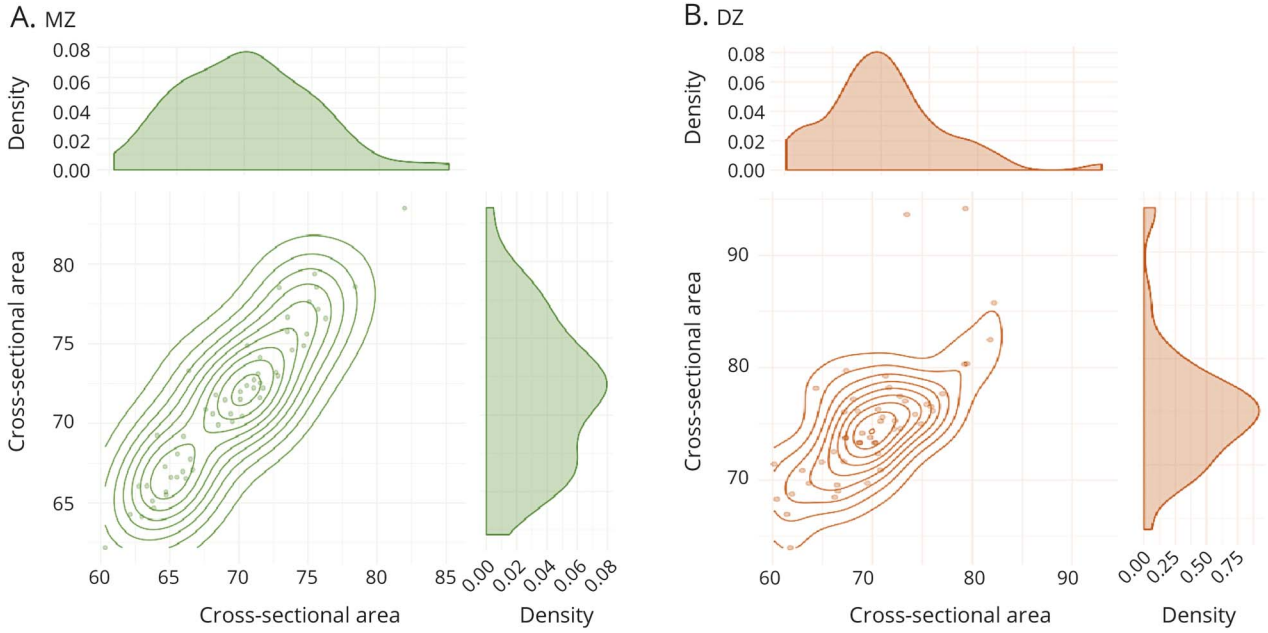

The segmented cord is marked in blue: (A) largest CSA in sample, 94.2 mm^2, (B) smallest CSA in sample, 60.2 mm^2, (C) largest ratio between LRW and APW (13.7 mm × 6.6 mm), and (D) smallest ratio between LRW and APW (10.4 mm × 9.1 mm). APW = anterior-posterior width; CSA = cross-sectional area; DZ = dizygotic; LRW = left-right width; MZ = monozygotic.

Figure 1 illustrates C2 anatomical results across the range of normal variation in the sample, and figure 2 demonstrates the extreme values regarding CSA and ratios between LRW and APW.

Heritability analysis

The AIC of the ACE and AE models for both the CSA APW measurements did not differ from each other, suggesting either model describes the data equally well. Comparing the AIC for the LRW measurement resulted in a lower log-likelihood ratio for the AE model, indicating that the AE model was a better fit for the data, where shared environment (C) had little influence. This is consistent with previous studies on brain structure.[24]

The AE model on CSA, LRW, and APW reported a broad-sense heritability of 0.912, 0.852, and 0.868, respectively; see also figure 3 for an illustration. See table 1 for model fitting parameter estimates and table 2 for heritability estimates.

Heritability of brain volume (no ventricles) was also carried out. The AIC suggested that the AE model was a better fit for the data. The AE model reported the broad-sense heritability of brain volume to be 0.955.

Correlations with physical, behavioral and brain measures

We investigated the relationship between CSA, LRW, and APW and (1) general physical measures, (2) motor behavior

Figure 3 Twin pair relationships of spinal cord CSA

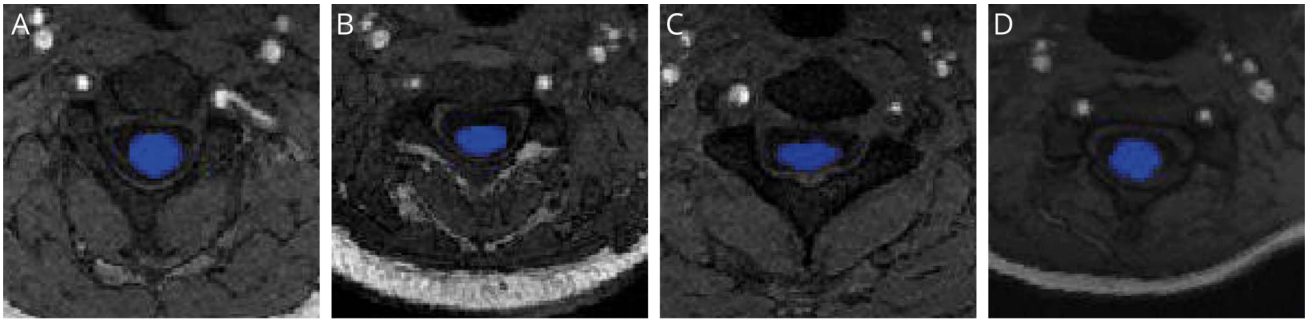

Correlations of CSA measures between each (A) MZ and (B) DZ twinset included in the analysis are illustrated, in addition to density plots showing the distribution of the data. CSA = cross-sectional area; DZ = dizygotic; MZ = monozygotic.

Table 1 Model fitting parameter estimates for analysis of heritability of spinal cord metrics and brain volume

							Variance estimates					
Measure	**Model**	**−2LL**	**df**	**AIC**	**χ^2**	***p* Value**	**a**	**95% CI**	**c**	**95% CI**	**e**	**95% CI**
CSA	ACE	−691.064	5	1,392.13			0.912	0.873–0.951	0.0	0.0 to 0.0	0.088	0.049–0.127
	AE	−691.064	4	1,390.13	<0.0001	1	0.912	0.873–0.951			0.088	0.049–0.127
APW	ACE	−124.405	5	258.81			0.868	0.810–0.926	0.0	0.0 to 0.0	0.132	0.074–0.190
	AE	−124.405	4	256.81		1	0.868	0.810–0.926			0.132	0.074–0.190
LRW	ACE	−181.56	5	373.112			0.822	0.398–1.246	0.3	−0.389 to 0.448	0.149	0.086–0.211
	AE	−181.569	4	371.139	0.019	0.8913	0.852	0.789–0.914			0.148	0.086–0.211
Brain volume	ACE	−2,993.46	4	5,994.926			0.597	0.369–0.825	0.359	0.128–0.590	0.044	0.025–0.063
	AE	−2,995.63	3	5,997.255	4.3294	0.0375	0.955	0.936–0.974			0.045	0.026–0.065

Abbreviations: −2LL = −2 log-likelihood; a = additive genetics; ACE = additive plus common plus nonshared environment and error model; AE = additive plus nonshared environment and error model; AIC = Akaike information criterion; APW = anterior-posterior width; c = shared environment; CI = confidence interval; CSA = cross-sectional area; df, degrees of freedom; e = unique environment; LRW = left-right width.

measures, and (3) regional brain measures (see supplementary table e-2, links.lww.com/NXG/A225). Aside from sex, which had a significant influence on several of the models, the only significant coefficients in the general physical models were CSA, LRW, and APW in relation to total brain volume ($p = 1.7 \times 10^{-12}$, 4.2×10^{-5}, and 3.4×10^{-7}, respectively) and a significance between height and LRW ($p = 0.00027$), where LRW increased proportionally with height of the participant.

In the behavioral models, there were no significant relationships. In the regional brain metrics models, whole brain volume was a significant covariate. Significant relationships were observed between CSA and thalamus volume ($p = 0.005$) and CSA and the occipital area; the CSA increased with the volume of the thalamus, whereas on the other hand, CSA was decreased proportional to the area of the occipital cortex ($p = 0.001$).

Sex as a biological variable

There was a significant difference in the CSA between men and women (73.57 vs 70.88 mm^2; $t = 3.86$; $p < 10^{-4}$) and in APW (8.18 vs 7.92 mm; $t = 4.43$; $p < 10^{-4}$), but not in the LRW (11.55 vs 11.50 mm; $t = 0.62$; $p = 0.5347$).

A multiple linear regression was calculated to predict CSA based on sex, body length, and weight, controlling for twin status A significant regression equation was found ($F(5,277) = 4.23$, $p < 0.001$), with an R^2 of 0.07. Predicted CSA is equal to 51.08 mm^2 − 1.3 (SEX) + 0.3 (HEIGHT) − 0.007 (WEIGHT), where sex is coded as 0 = Male, 1 = Female,

Table 2 Broad-sense heritability and within-twin correlations for each model of spinal cord and brain volume heritability analyses

Measure	**Model**	**Correlation within MZ**	**95% CI**	**Correlation within DZ**	**95% CI**	**h^2**
CSA	ACE	0.912	0.864–0.944	0.456	0.436–0.475	0.912
	AE	0.912	0.864–0.944	0.456	0.436–0.475	0.912
APW	ACE	0.868	0.797–0.915	0.434	0.405–0.462	0.868
	AE	0.868	0.797–0.915	0.434	0.405–0.462	0.868
LRW	ACE	0.852	0.775–0.903	0.441	0.208–0.626	0.822
	AE	0.852	0.776–0.903	0.426	0.394–0.457	0.852
Brain volume	ACE	0.956	0.933–0.972	0.658	0.523–0.760	0.597
	AE	0.955	0.931–0.970	0.477	0.468–0.487	0.955

Abbreviations: a = additive genetics; ACE = additive plus common plus nonshared environment and error model; AE = additive plus nonshared environment and error model; APW = anterior-posterior width; c = shared environment; CI = confidence interval; CSA = cross-sectional area; DZ = dizygotic; e = unique environment; h^2 = heritability; LRW = left-right width; MZ = monozygotic.

height is measured in inches, and weight is measured in pounds. Only body length was a predictor of CSA ($p = 0.02$, see table e-1, links.lww.com/NXG/A225).

A multiple linear regression was calculated to predict LRW based on sex, body length, and weight, controlling for twin status A significant regression equation was found ($F(5,277) = 2.92$, $p = 0.013$), with an R^2 of 0.05. Predicted LRW diameter is equal to 7.81 mm + 0.2 (SEX) + 0.05 (HEIGHT) − 0.0001 (WEIGHT), where sex is coded as 0 = Male, 1 = Female, height is measured in inches, and weight is measured in pounds. Only body length was a significant predictor of LRW diameter.

A multiple linear regression was calculated to predict APW based on sex, body length, and weight, controlling for twin status A significant regression equation was found ($F(5,277) = 4.04$, $p = 0.001$), with an R^2 of 0.07. Predicted APW diameter is equal to 8.13 mm − 0.27 (SEX) + 0.002 (HEIGHT) − 0.0007 (WEIGHT), where sex is coded as 0 = Male, 1 = Female, height is measured in inches, and weight is measured in pounds. Sex was the only significant predictor of APW diameter.

Discussion

In a young and healthy cohort, cervical spinal cord structure is quantifiable using semiautomated and unbiased methods from brain imaging data. Cervical spinal cord structure is highly heritable, with genetic influences ranging from 85% to 91%. C2 cervical CSA is linearly proportional to total brain volume and thalamus volume but is not related to height, weight, BMI, or measures of motor behavior in this sample.

Our estimates indicate a genetic component accounting for 91% of the variation in spinal cord CSA, 85% for LRW, and 87% for APW. This suggests that the level of genetic influence on spinal cord structure is comparable with what has been reported on brain volume (see reference 11 for a review). This suggests that genes play a bigger role in spinal cord structure compared with the nonpathological environment. We also did not observe any relationships to motor behavior in young healthy controls. As such, the large reductions in CSA consistently observed after SCI and in neurodegenerative states are not likely to be confounded by environmental factors before the onset of the disease. This makes them useful in tracking disease severity and progression.

The heritability analyses showed that shared environmental influence (the C component in the ACE model) had close to no influence in the 3 different measurements. The lack of influence by a shared environment could be because of the assumption that both DZ and MZ twins share a more similar environment, both in utero and in childhood, compared with nontwin family members.

The HCP sample showed an average C2 CSA of 71.77 mm^2 (n = 283), LRW of 11.52 mm, and an APW of 8.0 mm. Previous studies have shown large variations in the cervical CSA of healthy populations, ranging from 70.2[25] and 79.9[26] to 84.7 mm^2.[15] Our results are comparable with previous studies using the same segmentation method.[27] Postmortem studies have found C2 CSA to be between 56 ± 3.4 mm^2,[28] 70 ± 20 mm^2,[29] and 83 mm^2.[30] Data acquisition methods, such using T1- or T2-weighted images[31] and data analytical methods[25] influence the measures of cord anatomy.

The methods implemented in the Spinal Cord Toolbox have been validated elsewhere,[31] but here, we had the opportunity to test the reproducibility with a test-retest data set of 36 participants. Our analyses resulted in an intraclass correlation coefficient measure that is considered good to excellent for CSA and excellent for LRW and APW. Thus, the Spinal Cord Toolbox proves to be a reliable tool for estimating C2 CSA, LRW, and APW from T1-weighted magnetisation prepared rapid gradient echo data, even when C2 is close to the edge of the field of view, if gradient nonlinearity is accounted for. Because our measures displayed high test-retest reliability, the numerical differences in the literature may be due to the differences in MRI contrast between CSF and white matter dependent on imaging sequences, voxel size, scanner gradients, and differences in segmentation protocols. We recommend caution when pooling data from multiple sites or multiple imaging sequences. Correction for gradient nonlinearity is crucial (see appendix e-1, links.lww.com/NXG/A225). Dedicated spinal cord sequences isocentered over the spine and not the brain, and usage of both T1- and T2-weighted images improve generalizability.

Our analyses showed that CSA, LRW, and APW all significantly correlated with brain volume. Previous studies have also reported a relationship between cervical CSA and brain volume[26,32] or, in postmortem studies, between CSA and brain weight.[28] We also observed a relationship between LRW and body height, where LRW increased with height. This is in line with a previous study reporting a positive relationship between C7 CSA and body height in specimens from 152 cadavers.[28] However, no such relationship was observed in a study encompassing CT scans of 36 participants.[33]

We did not observe any further correlations between cord metrics and other physical features or motor behavior. The only regional brain metric that was correlated with CSA was thalamus volume and, surprisingly, an inverse relationship between CSA and occipital area. Given the number of ascending spinal cord tracts projecting to the thalamus, this relationship is plausible. The negative relationship between cord CSA and occipital area is more surprising and may be because of multicollinearity between occipital area and total brain volume.

As in previous studies,[26,34] men had significantly higher CSA than women and also higher LRW and APW. Notably, in multiple regression models, body length was the only predictor of CSA and LRW, whereas sex was the only predictor

of APW. It has been suggested that LRW is reflective of motor tracts mainly located in the lateral funiculi, whereas APW is reflective of the sensory tracts found in the dorsal funiculus.[35] Indeed, we found that LRW and APW were not proportional and thus largely independent metrics of cord anatomy. Previous studies indicate that tactile spatial acuity improves with decreasing finger size independent of sex[36] and that fingertips have a similar number of Meissner corpuscles, regardless of size.[37] As such, the number of fingertip sensory axons at C2 would be similar for a small and a large hand (or, in effect, for a short and a tall person). If this extrapolation holds for the whole body, it would suggest that the total number of sensory receptors and associated spinal axons are roughly equivalent across men and women and across body size but with higher density in smaller bodies. The observed relation between body length and cord diameter would then be reflective of the average axonal diameter, rather than the number of axons. Because axonal conduction velocity in myelinated axons is approximately linearly proportional to axon diameter,[38] we speculate that the observed cord-thickness body-length relationship is reflective of increased axonal diameter to achieve similar transmission times in short and tall bodies.

Owing to the narrow age range in the HCP young adult sample, we did not evaluate age effects. Previous studies are mixed, with reports of no correlation with age, height, and weight,[33] as well as reports of a relationship between spinal cord CSA and age and height.[39]

Previous studies in the spinal cord injured population have demonstrated parallel changes in both cord CSA and somatosensory regions[7,40,41] between CSA and hand grip strengths,[18] and between LRW and motor score,[35] whereas APW correlated with sensory scores.[35] In patients with MS, atrophy of the upper cervical cord is evident in APW but not LRW,[42] whereas studies on ALS have only reported on CSA.[3] We did not observe any relationships between motor function and cord metrics in the present large, young, and healthy cohort. This suggests that it might only be in pathologic states with anterograde and retrograde degeneration of white matter, reducing cord area by 5–22 mm^2, that such relationships are unmasked.

Several large imaging studies in MS have demonstrated extensive cord atrophy.[42–44] We also know from longitudinal neuroimaging studies that brain volume decreases with aging and in neurodegenerative disorders such as Alzheimer and Parkinson disease. Whether the CSA of the spinal cord changes over time in healthy individuals is inconclusive.[45] Some studies have found small reductions in the spinal cord CSA in elderly individuals.[46–48] Future studies should aim to elucidate the changes in spinal cord structure in healthy and pathologic aging and if it correlates with changes in motor and sensory functioning. Several ongoing brain neuroimaging efforts have an adequate field of view to evaluate developmental and neurodegenerative effects on the upper cervical cord. This will provide additional meaningful metrics both for clinical and scientific examination.

Some caution should be exercised when interpreting the spinal cord imaging studies because the spinal cord is a relatively small area and is susceptible to partial volume effects. HCP data were collected using 0.7 × 0.7 × 0.7 mm resolution, a substantial improvement over typical 1-mm isotropic data but much higher resolution methods are being developed.[49] Moreover, signal-to-noise ratio at the outer edges of the field of view (i.e., in the spine area of a brain scan) can be low, making a segmentation based on intensities more challenging. However, the C2 spinal cord level is an optimal region to study because there is very little curvature, making a distinction between the spinal cord and surrounding CSF easier.[15]

Another limitation on the analytic level is the use of the AE model. The AE model gives estimation pertaining to 2 factors: additive genetic effect (A) and unique environmental effect (E). It is noted that the E term also absorbs variation that arises from measurement error and individual day-to-day fluctuations. Linear mixed effects models that explicitly account measurement errors by using repeated measures have been developed[50] but were not used here because our test-retest sample was deemed too small.

Similar to the brain, cervical spinal cord anatomy is highly heritable. Provided that the field of view is sufficient to cover the first 2–3 vertebrae, C2 CSA, LRW, and APW can reliably be measured in brain dedicated neuroimaging protocols. With large data sharing initiatives, this opens the possibility to examine these relatively unexplored metrics that harbor important markers of development and pathology.

Acknowledgment

Data were provided by the Human Connectome Project, WU-Minn Consortium (Principal Investigators: David Van Essen and Kamil Ugurbil; 1U54MH091657) funded by the 16 NIH Institutes and Centers that support the NIH Blueprint for Neuroscience Research and by the McDonnell Center for Systems Neuroscience at Washington University.

Study funding

Research reported in this publication was supported by the Promobilia Foundation, Wings for Life, The Gordon Foundation (C. Linnman), the Department of Defense SC140194 (C. Linnman, L. Solstrand Dahlberg), NICHD of the NIH under award number 1R01HD097407 (C. Linnman), and the BRAIN *Initiative* (NIMH grant R01-MH111419) (O. Viessmann).

Disclosure

Disclosures available: Neurology.org/NG.

Publication history

Received by *Neurology: Genetics* May 17, 2019. Accepted in final form January 13, 2020.

Appendix 1 Authors

Name	Location	Role	Contribution
Linda Solstrand Dahlberg, PhD	Harvard Medical School, MA	Author	Analyzed the data, data interpretation, and drafted the manuscript
Olivia Viessmann, PhD	Harvard Medical School, MA	Author	Processed the data and revised the manuscript for intellectual content
Clas Linnman, PhD	Harvard Medical School, MA	Author	Conceptualized the study, analyzed the data, data interpretation, and drafted the manuscript

References

1. Rashid W, Davies GR, Chard DT, et al. Increasing cord atrophy in early relapsing-remitting multiple sclerosis: a 3 year study. J Neurol Neurosurg Psychiatry 2006;77:51–55.
2. Abdel-Aziz K, Schneider T, Solanky BS, et al. Evidence for early neurodegeneration in the cervical cord of patients with primary progressive multiple sclerosis. Brain 2015;138:1568–1582.
3. El Mendili M-M, Cohen-Adad J, Pelegrini-Issac M, et al. Multi-parametric spinal cord MRI as potential progression marker in amyotrophic lateral sclerosis. PLoS One 2014;9:e95516.
4. Filippi M, Rocca MA. Multiple sclerosis: linking disability and spinal cord imaging outcomes in MS. Nat Rev Neurol 2013;9:189–190.
5. Kearney H, Miller DH, Ciccarelli O. Spinal cord MRI in multiple sclerosis—diagnostic, prognostic and clinical value. Nat Rev Neurol 2015;11:327–338.
6. Lin X, Tench CR, Evangelou N, Jaspan T, Constantinescu CS. Measurement of spinal cord atrophy in multiple sclerosis. J Neuroimaging 2004;14:20S–26S.
7. Freund P, Weiskopf N, Ashburner J, et al. MRI investigation of the sensorimotor cortex and the corticospinal tract after acute spinal cord injury: a prospective longitudinal study. Lancet Neurol 2013;12:873–881.
8. Freund P, Curt A, Friston K, Thompson A. Tracking changes following spinal cord injury: insights from neuroimaging. Neuroscientist 2013;19:116–128.
9. Jurkiewicz MT, Crawley AP, Verrier MC, Fehlings MG, Mikulis DJ. Somatosensory cortical atrophy after spinal cord injury: a voxel-based morphometry study. Neurology 2006;66:762–764.
10. Wrigley PJ, Gustin SM, Macey PM, et al. Anatomical changes in human motor cortex and motor pathways following complete thoracic spinal cord injury. Cereb Cortex 2009;19:224–232.
11. Peper JS, Brouwer RM, Boomsma DI, Kahn RS, Hulshoff Pol HE. Genetic influences on human brain structure: a review of brain imaging studies in twins. Hum Brain Mapp 2007;28:464–473.
12. Glasser MF, Coalson TS, Robinson EC, et al. A multi-modal parcellation of human cerebral cortex. Nature 2016;536:171–178.
13. Glasser MF, Sotiropoulos SN, Wilson JA, et al. The minimal preprocessing pipelines for the Human Connectome Project. Neuroimage 2013;80:105–124.
14. De Leener B, Levy S, Dupont SM, et al. SCT: Spinal Cord Toolbox, an open-source software for processing spinal cord MRI data. Neuroimage 2017;145:24–43.
15. Losseff NA, Webb SL, O'Riordan JI, et al. Spinal cord atrophy and disability in multiple sclerosis: a new reproducible and sensitive MRI method with potential to monitor disease progression. Brain 1996;119:701–708.
16. Ziegler G, Grabher P, Thompson A, et al. Progressive neurodegeneration following spinal cord injury: implications for clinical trials. Neurology 2018;90:e1257–e1266.
17. Horsfield MA, Sala S, Neema M, et al. Rapid semi-automatic segmentation of the spinal cord from magnetic resonance images: application in multiple sclerosis. Neuroimage 2010;50:446–455.
18. Freund P, Weiskopf N, Ward NS, et al. Disability, atrophy and cortical reorganization following spinal cord injury. Brain 2011;134:1610–1622.
19. Reuben DB, Magasi S, McCreath HE, et al. Motor assessment using the NIH Toolbox. Neurology 2013;80:S65–S75.
20. Hur J, Iordan AD, Dolcos F, Berenbaum H. Emotional influences on perception and working memory. Cogn Emot 2017;31:1294–1302.
21. Carlin JB, Gurrin LC, Sterne JA, Morley R, Dwyer T. Regression models for twin studies: a critical review. Int J Epidemiol 2005;34:1089–1099.
22. Van Essen DC, Smith SM, Barch DM, Behrens TEJ, Yacoub E, Ugurbil K. The WU-Minn Human Connectome Project: an overview. Neuroimage 2013;80:62–79.
23. Motulsky HJ, Brown RE. Detecting outliers when fitting data with nonlinear regression - a new method based on robust nonlinear regression and the false discovery rate. BMC Bioinformatics 2006;7:123.
24. Hibar DP, Stein JL, Renteria ME, et al. Common genetic variants influence human subcortical brain structures. Nature 2015;520:224–229.
25. Yiannakas MC, Mustafa AM, De Leener B, et al. Fully automated segmentation of the cervical cord from T1-weighted MRI using PropSeg: application to multiple sclerosis. Neuroimage Clin 2016;10:71–77.
26. Papinutto N, Schlaeger R, Panara V, et al. Age, gender and normalization covariates for spinal cord gray matter and total cross-sectional areas at cervical and thoracic levels: a 2D phase sensitive inversion recovery imaging study. PLoS One 2015;10:e0118576.
27. De Leener B, Cohen-Adad J, Kadoury S. Automatic segmentation of the spinal cord and spinal canal coupled with vertebral labeling. IEEE Trans Med Imaging 2015;34:1705–1718.
28. Kameyama T, Hashizume Y, Ando T, Takahashi A. Morphometry of the normal cadaveric cervical spinal cord. Spine (Phila Pa 1976) 1994;19:2077–2081.
29. Ko H-Y, Park JH, Shin YB, Baek SY. Gross quantitative measurements of spinal cord segments in human. Spinal Cord 2004;42:35–40.
30. Donaldson HH, Davis DJ. A description of charts showing the areas of the cross sections of the human spinal cord at the level of each spinal nerve. J Comp Neurol 1903;13:19–40.
31. De Leener B, Kadoury S, Cohen-Adad J. Robust, accurate and fast automatic segmentation of the spinal cord. Neuroimage 2014;98:528–536.
32. Engl C, Schmidt P, Arsic M, et al. Brain size and white matter content of cerebrospinal tracts determine the upper cervical cord area: evidence from structural brain MRI. Neuroradiology 2013;55:963–970.
33. Yu YL, du Boulay GH, Stevens JM, Kendall BE. Morphology and measurements of the cervical spinal cord in computer-assisted myelography. Neuroradiology 1985;27:399–402.
34. Ulbrich EJ, Schraner C, Boesch C, et al. Normative MR cervical spinal canal dimensions. Radiology 2014;271:172–182.
35. Lundell H, Barthelemy D, Skimminge A, Dyrby TB, Biering-Sorensen F, Nielsen JB. Independent spinal cord atrophy measures correlate to motor and sensory deficits in individuals with spinal cord injury. Spinal Cord 2011;49:70–75.
36. Peters RM, Hackeman E, Goldreich D. Diminutive digits discern delicate details: fingertip size and the sex difference in tactile spatial acuity. J Neurosci 2009;29:15756–15761.
37. Dillon YK, Haynes J, Henneberg M. The relationship of the number of Meissner's corpuscles to dermatoglyphic characters and finger size. J Anat 2001;199:577–584.
38. Hursh JB. Conduction velocity and diameter of nerve fibers. Am J Physiol Content 1939;127:131–139.
39. Kameyama T, Hashizume Y, Sobue G. Morphologic features of the normal human cadaveric spinal cord. Spine (Phila Pa 1976) 1996;21:1285–1290.
40. Jutzeler CR, Huber E, Callaghan MF, et al. Association of pain and CNS structural changes after spinal cord injury. Sci Rep 2016;6:18534.
41. Hou J, Xiang Z, Yan R, et al. Motor recovery at 6 months after admission is related to structural and functional reorganization of the spine and brain in patients with spinal cord injury. Hum Brain Mapp 2016;37:2195–2209.
42. Lundell H, Svolgaard O, Dogonowski AM, et al. Spinal cord atrophy in anterior-posterior direction reflects impairment in multiple sclerosis. Acta Neurol Scand 2017;136:330–337.
43. Azodi S, Nair G, Enose-Akahata Y, et al. Imaging spinal cord atrophy in progressive myelopathies: HTLV-I-associated neurological disease (HAM/TSP) and multiple sclerosis (MS). Ann Neurol 2017;82:719–728.
44. Eden D, Gros C, Badji A, et al. Spatial distribution of multiple sclerosis lesions in the cervical spinal cord. Brain 2019;142:633–646.
45. Valsasina P, Rocca MA, Horsfield MA, Copetti M, Filippi M. A longitudinal MRI study of cervical cord atrophy in multiple sclerosis. J Neurol 2015;262:1622–1628.
46. Valsasina P, Horsfield MA, Rocca MA, Absinta M, Comi G, Filippi M. Spatial normalization and regional assessment of cord atrophy: voxel-based analysis of cervical cord 3D T1-weighted images. AJNR Am J Neuroradiol 2012;33:2195–2200.
47. Agosta F, Laganà M, Valsasina P, et al. Evidence for cervical cord tissue disorganisation with aging by diffusion tensor MRI. Neuroimage 2007;36:728–735.
48. Yanase M, Matsuyama Y, Hirose K, et al. Measurement of the cervical spinal cord volume on MRI. J Spinal Disord Tech 2006;19:125–129.
49. Zhao W, Cohen-Adad J, Polimeni JR, et al. Nineteen-channel receive array and four-channel transmit array coil for cervical spinal cord imaging at 7T. Magn Reson Med 2014;72:291–300.
50. Ge T, Holmes AJ, Buckner RL, Smoller JW, Sabuncu MR. Heritability analysis with repeat measurements and its application to resting-state functional connectivity. Proc Natl Acad Sci USA 2017;114:5521–5526.